The mechanistic basis for chromatin invasion and remodeling by the yeast pioneer transcription factor Rap1

Maxime Mivelaz[1], Anne-Marinette Cao[1], Slawomir Kubik[2,4], Sevil Zencir[2], Ruud Hovius[1], Iuliia Boichenko[1], Anna Maria Stachowicz[2], Christoph F. Kurat[3], David Shore[2] and Beat Fierz[1*]

[1] École Polytechnique Fédérale de Lausanne, SB ISIC LCBM, Station 6, CH-1015 Lausanne, Switzerland

[2] Department of Molecular Biology and Institute of Genetics and Genomics of Geneva (iGE3), 1211 Geneva 4, Switzerland

[3] Molecular Biology Division, Biomedical Center, Faculty of Medicine, LMU Munich, 82152 Planegg-Martinsried, Germany

[4] Current address: Sophia Genetics, Campus Biotech, 9 Chemin des Mines, 1202 Genève

*Corresponding author: beat.fierz@epfl.ch

Keywords: Rap1, pioneer transcription factor, chromatin structure, single-molecule fluorescence

SUMMARY

Pioneer transcription factors (pTFs) bind to target sites within compact chromatin initiating chromatin remodeling and controlling the recruitment of downstream factors. The mechanisms by which pTFs overcome the chromatin barrier are not well understood. Here we reveal, using single-molecule fluorescence, how the yeast transcription factor Rap1 invades and remodels chromatin. Using a reconstituted chromatin system replicating yeast promoter architecture we demonstrate that Rap1 can bind nucleosomal DNA within a chromatin fiber, but with shortened dwell times compared to naked DNA. Moreover, we show that Rap1 binding opens chromatin fiber structure by inhibiting inter-nucleosome contacts. Finally, we reveal that Rap1 collaborates with the chromatin remodeler RSC to displace promoter nucleosomes, paving the way for long-lived bound states on newly exposed DNA. Together, our results provide a mechanistic view of how Rap1 gains access and opens chromatin, thereby establishing an active promoter architecture and controlling gene expression.

Chromatin acts as a barrier for proteins which require access to DNA. Both target search and binding-site recognition of transcription factors (TFs) are restricted by the presence of nucleosomes and chromatin higher-order structure (Adams and Workman, 1995; Mirny, 2010). However, a subset of transcription factors, named 'pioneer transcription factors' (pTFs) (Zaret and Mango, 2016), have the ability to invade compact chromatin domains. This initiates an opening of chromatin structure (Cirillo et al., 2002; Fakhouri et al., 2010), which can coincide with linker histone loss (Iwafuchi-Doi et al., 2016) or nucleosome removal (Jin et al., 2009; Knight et al., 2014; Suto et al., 2000). Such remodeled chromatin is accessible to subsequent non-pioneer TFs (Cirillo et al., 2002), which together produce changes in transcriptional programs (Soufi et al., 2015; Zaret and Carroll, 2011).

A common feature of DNA binding domains (DBDs) found in pTFs is their ability to bind partial sequence motifs displayed on nucleosomes (Soufi et al., 2015). The presence of nucleosomes may therefore have limited effects on both on-rates and residence times of pTFs. Beyond the nucleosome,

higher-order chromatin structure further constrains DNA conformation and accessibility (Poirier et al., 2008). High-resolution structural studies on reconstituted chromatin revealed that local structural elements such as tetranucleosome units form the basis of chromatin fiber organization (Schalch et al., 2005). Neighboring tetranucleosome units can interact and form fiber segments with two intertwined stacks of nucleosomes (Li et al., 2016; Schalch et al., 2005; Song et al., 2014). Importantly, genomic studies have confirmed the prevalence of tetranucleosome contacts *in vivo* (Hsieh et al., 2015; Risca et al., 2017). Such higher-order structure may further restrict DNA access.

It is not well understood how pTFs probe DNA sequences within chromatin and how they invade and subsequently remodel chromatin structure. The intrinsic dynamics of chromatin itself might provide a potential mechanism for pTF invasion (Cuvier and Fierz, 2017). Recent studies using force spectroscopy (Li et al., 2016) or single-molecule FRET (Kilic et al., 2018b) revealed conformational dynamics in chromatin fibers from microseconds to seconds. It is thus conceivable that pTFs exploit dynamic site exposure within chromatin fibers to invade compact chromatin, where they then recruit additional cellular machinery to enact necessary conformational reorganization to alter gene expression (**Figure 1a**).

Here, we test this hypothesis and reveal the mechanism of chromatin invasion, target binding and chromatin remodeling of the pTF Rap1 (repressor activator protein 1). Rap1 is an important general regulatory factor (GRF) of transcription in budding yeast (Knight et al., 2014). It plays multiple roles *in vivo* including the transcriptional regulation of around 5% of yeast genes (Lieb et al., 2001), repression of noncoding transcripts (Challal et al., 2018; Wu et al., 2018) and the maintenance of telomeric integrity (Wellinger and Zakian, 2012). The Rap1 DNA binding domain (DBD) consists of dual Myb-type domains which are connected by a short unstructured linker (Konig et al., 1998) (**Figure 1b**). The DBD binds a class of 13 bp consensus motifs with high affinity (**Figure S1a**), only requiring direct access to one face of the DNA (**Figure 1b**). Importantly, Rap1 can engage a single motif in multiple binding modes, involving one or both Myb-domains (Feldmann and Galletto, 2014). Moreover, Rap1 has previously been identified as being able to bind nucleosomes *in vitro* (Rossetti et al., 2001). In the

cell, Rap1 binding sites are located within nucleosome-depleted regions (NDR) upstream of the transcription start site (TSS), or within the -1 nucleosome at the two most peripheral exposed DNA major grooves (Koerber et al., 2009). A host of cell-based studies showed that Rap1 binding at these loci results in chromatin opening (Yu and Morse, 1999), nucleosome loss and NDR formation (Badis et al., 2008; Kubik et al., 2015; van Bakel et al., 2013; Yan et al., 2018). In fact, NDRs are typical for most active eukaryotic promoters (Jiang and Pugh, 2009), and depend on the action of remodeling factors, including RSC (Badis et al., 2008; Brahma and Henikoff, 2018; Cairns et al., 1996; Hartley and Madhani, 2009; Kubik et al., 2018; Ng et al., 2002; Parnell et al., 2008), SWI/SNF (Rawal et al., 2018; Yen et al., 2012) and INO80 (Krietenstein et al., 2016).

A particularly important gene family co-regulated by Rap1 are ribosomal protein genes. Rap1 binds to the promoter/enhancer regions of >90% of these genes and initiates the recruitment of additional TFs, including Hmo1, Fhl1 and Ifh1 (Knight et al., 2014). In one of the two largest categories of ribosomal protein genes (category I), two closely spaced Rap1 binding sites are situated in the NDR upstream of the TSS (Knight et al., 2014). In contrast, when Rap1 is depleted, its binding sites are covered by a stable nucleosome (Kubik et al., 2015). Digestion of yeast chromatin with limited amounts of micrococcal nuclease (MNase) followed by sequencing (MNase-seq) (Zentner and Henikoff, 2012) revealed that many NDRs contain MNase-sensitive particles (Henikoff et al., 2011; Kent et al., 2011; Weiner et al., 2010; Xi et al., 2011), which may correspond to destabilized promoter nucleosomes (Brahma and Henikoff, 2018; Chereji et al., 2017; Kubik et al., 2017; Kubik et al., 2015; Kubik et al., 2018). In category I promoters such MNase sensitive nucleosome-like particles appear upstream of the +1 nucleosome, co-existing with bound Rap1 (Kubik et al., 2015). In summary, Rap1 is a well characterized factor that directly impacts chromatin organization at key genes. However, the molecular mechanism by which Rap1 finds its target in compacted chromatin and by which it subsequently acts to open chromatin and displaces promoter nucleosomes is not understood.

To reveal dynamic Rap1 invasion mechanisms, we reconstituted nucleosomes and chromatin fibers containing Rap1 binding sites in the configuration found in category I promoters. We find that

the residence times, but not binding rates, of Rap1 are strongly reduced by the presence of nucleosomes and chromatin fiber structure. We show that Rap1 binding does not disrupt or decidedly alter nucleosome structure. In contrast, single-molecule FRET measurements directly reveal that Rap1 locally opens chromatin fiber structure. Finally, we demonstrate that Rap1 collaborates with RSC to displace nucleosomes from their target sites. The remodeled chromatin structure then provides an opening for stable Rap1 binding, access to further transcription factors and finally gene regulation.

RESULTS

Rap1 binds to nucleosomes via non-specific and specific DNA interactions

In a first set of experiments we investigated the mechanism of nucleosome binding by Rap1. We chose the ribosomal protein L30 (*RPL30*) promoter (category I) as our target for this study (**Figure 1c**). Using MNase-seq under Rap1-depleted conditions, we mapped the position of the -1 nucleosome (**Figure 1c**), which contains two Rap1 binding sites and which is displaced *in vivo* upon Rap1 binding (Kubik et al., 2015). Within this nucleosome, Rap1 binding site 1 (*S1*) is located near super helical location (SHL) 4.5, whereas site 2 (*S2*) resides near the DNA entry-exit site at SHL 6.5 (**Figure 1d**). Importantly, the affinity of Rap1 for the two sites is distinct with a dissociation constant K_d of ~10 nM for *S1* and ~30 nM for *S2* (as determined by electromobility shift assays (EMSA), **Figure S1c-e**). *In vivo,* both sites contribute to the expression of the *RPL30* gene product (Knight et al., 2014).

To directly observe dynamic Rap1 binding to promoter nucleosomes, we used a single-molecule total internal reflection fluorescence microscopy approach (smTIRFM) that reveals TF binding to immobilized DNA, nucleosomes or chromatin segments via fluorescence colocalization (**Figure 2a**) (Kilic et al., 2015). Several reagents were required: first, we generated a 235 base pair (bp) DNA template based on the 601 nucleosome positioning sequence (Thastrom et al., 1999), which contained one or both Rap1 binding sites, *S1* or *S2,* at the same nucleosome position as in the native promoter (**Figure 1d**, **Figure S1b** and **Table S2-4**). Moreover, the DNA constructs contained a far-red fluorescent dye (Alexa Fluor 647) and a biotin moiety for immobilization. We then either used this DNA directly or

reconstituted nucleosomes using recombinantly expressed histones (**Figure 2a** and **Figure S2a-e**). Second, we purified full-length Rap1 as a Halo-tag fusion from insect cells and fluorescently labeled the protein with the highly photostable green-orange dye JF-549 (Grimm et al., 2015) (**Figure 2b, Figure S2f-k**). Importantly, labeled Rap1 exhibited similar DNA binding compared to published values (Knight et al., 2014) (**Figure S1c-e**).

Having all components in hand, in a first set of experiments we immobilized *S1*- or *S2*-containing naked DNA in a microfluidic channel and determined their position by smTIRFM imaging in the far-red channel (**Figure 2c**). We then injected Rap1 at a concentration chosen such that individual, non-overlapping binding events could be detected as fluorescent spots in the green-orange channel (usually 50-100 pM). Colocalization of Rap1 detections with DNA positions indicated binding (**Figure 2c**). We then recorded movies which revealed the binding kinetics of Rap1 to *S1*- or *S2*-containing naked DNA. For each DNA molecule, extracted kinetic traces allowed us to determine the length of individual binding events (t_{bright}) and intermittent search times (t_{dark}). The effect of dye photobleaching on residence time measurements was reduced by stroboscopic imaging (**Figure S3a**).

While dynamic Rap1 binding was observed for the medium affinity site *S2* (**Figure 2d**), individual binding events to the high affinity site *S1* were so long (> 40 min) that we were not able to obtain suitable statistics (**Figure S3b**). For *S2*-containing DNA, we then constructed cumulative lifetime histograms of bright times (t_{bright}) (**Figure 2e**), which were fitted using a bi-exponential function, yielding two residence times $\tau_{off,1}$ and $\tau_{off,2}$ (**Figure 2f**, see **Table S1** for all rate constants). Of all binding events, 35% exhibited a short residence time ($\tau_{off,1}$ = 12.4 ± 4.5 s) whereas the remaining 65% showed slow Rap1 dissociation kinetics ($\tau_{off,2}$ = 452 ± 115 s). Due to the dual Myb-type DBD, these different residence times may indicate different binding modes where either the entire or only a partial DNA binding motif is engaged. Under equilibrium binding conditions, Rap1 thus forms long-lived complexes with free DNA, resulting in residence times in the minutes to hours range for *S1* and *S2*.

In contrast, the presence of mononucleosomes (MNs) shortened the residence time of Rap1, as observed in kinetic traces for MNs containing either *S1* or *S2* (**Figure 2g**), and in the corresponding

lifetime histograms (**Figure 2h**). Here, a tri-exponential function was required to describe the data (**Figure S3c-e**). Around 50% of all detected events were short-lived, with a time constant of $0.2 < \tau_{off,0} < 0.7$ s. We attribute these fast events to non-specific probing interactions of nucleosomal DNA. Rap1 binding to *S1* or *S2* further revealed two additional longer time constants $\tau_{off,1}$ and $\tau_{off,2}$: Rap1 binding to the high affinity site *S1* was associated with longer residence times ($\tau_{off,1}$ = 18 ± 11 s and $\tau_{off,2}$ > 100 s) compared to *S2* ($\tau_{off,1}$ = 8.4 ± 1.4 s, $\tau_{off,2}$ = 46 ± 3 s) (**Figure 2f**). This is not necessarily expected, as *S1* is located further within the nucleosome structure and thus potentially less accessible than *S2*, which resides at the DNA entry-exit site. To test the effect of site positioning on the nucleosome, we moved *S2* from SHL 6.5 to SHL 4.5. This resulted in an additional reduction in Rap1 residence time to $\tau_{off,1}$ = 2.4 ± 0.4 s and $\tau_{off,2}$ = 7.7 ± 1.9 s (**Figure S3f-h**). Of note, having both sites *S1* and *S2* in the same nucleosomes resulted in a superposition of the individual binding kinetics under our measurement conditions (**Figure S3i,j**).

Specific binding rates (k_{on}) that were obtained from analyzing lifetime histograms of dark times (t_{dark}) (**Figure S3k-m**) were comparable for all DNA and nucleosome constructs analyzed (**Figure 2i**). This demonstrates that the Rap1 target search kinetics are not influenced by the presence of nucleosomes. Finally, we also probed Rap1 binding to nucleosomes without binding sites (**Figure S3n-p**). A majority (83%) of all detected binding events were shorter than a second while the remaining 17% persisted for only 3.5 ± 3 s, consistent with nonspecific nucleosome interactions (**Figure 2f,i**). Together, these results indicate that Rap1 can bind to nucleosomal DNA, with overall similar on-rates and with reduced residence times (> 10-fold) compared to free DNA, which depend on the site position on the nucleosome.

Chromatin structure shortens Rap1 dwell times

In the cell, pTFs have to invade compact chromatin structure, which has been shown to reduce pTF accessibility (Soufi et al., 2012). We therefore proceeded to investigate the mechanism of dynamic chromatin structure invasion by Rap1. To this end, we employed a modular system to construct

chromatin fibers (Kilic et al., 2018b), based on a 12-mer repeat of 601 nucleosome positioning sequence each separated by 30 bp of linker DNA. We assembled two chromatin fiber types, containing Rap1 target sites *S1* or *S2* in their central nucleosome (N6) in the same orientation as within the *RPL30* promoter (**Figure 3a**, **Figure S4a-h**). The chromatin fibers were then immobilized in a flow cell and Rap1 binding dynamics were determined using smTIRFM (**Figure 3b**). Importantly, under our measurement conditions (130 mM KCl), chromatin fibers exist in a compact state (Allahverdi et al., 2015) (see also below).

Compared to MNs, we observed an increase in short (0.6 s) Rap1 binding events on chromatin fibers (~70% of all detections, **Figure 3c**), which can be attributed to non-specific probing interactions. Rap1 thus rapidly samples the chromatin fiber in its search for potential target sites. For fibers containing Rap1 binding sites (but not for chromatin devoid of such, **Figure S4i-k**), additional longer-lived binding events were detected (**Figure 3c**). This demonstrates that Rap1 can indeed invade compact chromatin fibers. Analyzing the lifetime histograms for *S2*- (**Figure 3d**) or *S1*- (**Figure 3e**) containing fibers revealed two time constants for specific interactions (**Figure S4l-m**). This is similar to the situation in MNs, reflecting multiple Rap1 binding modes. The Rap1 residence times were however further reduced in chromatin fibers (**Figure 3f**), by about 3-fold for *S2* ($\tau_{off,1}$ = 2.6 ± 0.6 s, and $\tau_{off,2}$ = 16.8 ± 3 s) and 5-fold for *S1* ($\tau_{off,1}$ = 3.2 ± 0.6 s, and $\tau_{off,2}$ = 25.6 ± 4.0 s). This shortening of Rap1 dwell times demonstrates that chromatin fiber structure acts as an additional hindrance to Rap1 binding.

To determine if chromatin also inhibits the target search process of Rap1 we investigated the on-rates (k_{on}) in chromatin compared to nucleosomes. Surprisingly, we could not detect any significant reduction in the Rap1 binding rate for chromatin fibers containing *S1* or *S2* (**Figure 3g**). It is thus conceivable that Rap1 can hop or slide along chromatin in search of the appropriate binding site, using non-specific DNA interactions as a means of chromatin anchoring. Chromatin dynamics on the millisecond time-scale (Kilic et al., 2018b) will eventually expose internal DNA sites, allowing the factor to bind to its target sequence with similar kinetics compared to naked DNA.

Rap1 binding does not evict or distort bound nucleosomes

Having established that Rap1 indeed binds to nucleosomes and can invade chromatin structure, we wondered if the pTF can remodel chromatin, i.e. by directly opening chromatin structure (Zaret and Carroll, 2011). In cells, Rap1 binding results in the destabilization and disruption of promoter nucleosomes (Knight et al., 2014; Kubik et al., 2015; van Bakel et al., 2013; Yan et al., 2018), thereby paving the way for binding of subsequent TFs and establishing a chromatin state permissive to transcription. First, we wondered if Rap1 association directly destabilizes nucleosome structure, and leads to DNA unwrapping as observed for other TFs (Donovan et al., 2019; Li et al., 2005; Li and Widom, 2004; Luo et al., 2014). We therefore established a FRET-based assay to monitor nucleosomal DNA unwrapping (**Figure 4a, Figure S5a-d**). We positioned FRET donor (Alexa568) and acceptor (Alexa647) dyes within the linker DNA of *S1*- and *S2*-containing nucleosomes, such that partial DNA unwrapping (or nucleosome disassembly) will lead to FRET loss (**Figure 4a,b, Figure S5d**). Upon Rap1 addition (from 1 to 10 equivalents (eq.)) nucleosomes were bound, as judged by EMSA (**Figure 4c**). However, no change in FRET efficiency (E_{FRET}) was observed for either *S1* or *S2* nucleosomes (**Figure 4d,e**), even at the highest Rap1 concentrations (**Figure 4f**). These experiments directly show that Rap1 binding to *S1* or *S2* does not dramatically affect nucleosome structure and does not result in DNA unwrapping or histone loss. We further tested if Rap1 shows affinity differences for nucleosomes, when its binding site is moved in 3 bp steps around the DNA helix. Indeed, Rap1 bound to *S1* with a K_d of ~80 nM, with ~50 nM for *S1* shifted by 3 bp, and ~60 nM for *S1* shifted by 6 bp (**Figure S5e-g**). These rotational affinity differences are consistent with Rap1 binding on the nucleosome surface.

Importantly, nucleosomes formed using the native *RPL30* DNA sequence also remained stable upon Rap1 binding (**Figure S5h-j**). Performing ensemble FRET experiments for such *RPL30* nucleosomes yielded overall lower FRET values compared to 601 derived sequences as the nucleosomes were less well positioned, but Rap1 binding did not result in a loss in FRET (**Figure S5k-m**). Finally, single-molecule Rap1 binding experiments using *RPL30* nucleosomes containing site *S1* revealed comparable residence times to 601 nucleosomes (**Figure S5n-q**) and no progressive loss of nucleosomes was observed (**Figure**

S5p). Together, these experiments demonstrate that Rap1 binding in itself does not greatly distort or disrupt nucleosome structure.

Rap1 locally opens chromatin structure

While the structure of individual nucleosomes is not disrupted by Rap1 binding, higher-order chromatin structure might be altered. We thus performed single-molecule FRET (smFRET) experiments which directly report on nucleosome stacking interactions (Kilic et al., 2018a; Kilic et al., 2018b). We inserted a Rap1 binding site (*S2*) in the central nucleosome (N6) in a 12-mer chromatin fiber, flanked by nucleosomes carrying a FRET donor (Cy3B in N5) and acceptor dye (Alexa647 in N7) (**Figure 5a**, **Figure S6a-g**). As a control, we also produced fibers without a binding site (no site, *NS*).

First, we characterized the conformations exhibited by these chromatin fibers by measuring E_{FRET}, which reports on the inter-nucleosome distance. High E_{FRET} values indicate compact chromatin, whereas a reduction in E_{FRET} reveals a loss in higher-order structure (e.g. due to unstacking of a tetranucleosome unit). We immobilized fibers in a flow channel and recorded movies under smTIRF conditions (**Figure 5b**). From the resulting time traces (**Figure 5c,d**) we constructed FRET histograms and fitted them using 3 Gaussian functions (**Figure 5e,f**). At native ionic strength (150 mM KCl), we observed a major population at high FRET (HF) (E_{FRET} ~ 0.5), as well as minor populations at medium (MF, E_{FRET} ~ 0.3) and low FRET (LF) (E_{FRET} < 0.1) (**Figure 5c-f**). Similar values were obtained in the presence of divalent cations (4 mM Mg^{2+}) which induce compact chromatin (**Figure S6h-o**) (Dorigo et al., 2003). In contrast, at low ionic strength (40 mM KCl) where chromatin is open, the HF population was absent, and only the MF state was observed. Together, these measurements enabled us to assign the HF state to compact chromatin and nucleosome stacking, whereas the MF state reflects open chromatin. Finally, the LF state is observed for all fibers and indicates chromatin assembly defects (e.g. shifted or lacking nucleosomes at dye positions) (Kilic et al., 2018b), and is thus disregarded for the analysis.

We could now probe the effect of Rap1 invasion on chromatin fibers. We thus titrated Rap1 onto chromatin fibers with (*S2*) or without (*NS*) a Rap1 binding site, using concentrations from 50 – 500 pM. For *S2*-containing fibers the fraction of tightly compacted chromatin (the HF population) was reduced, and locally opened chromatin (MF) was populated with increasing Rap1 concentration (**Figure 5e,g**). In contrast, chromatin lacking Rap1 binding sites was not sensitive to Rap1 addition (**Figure 5f,h**). Moreover, a subset (~18-25%) of FRET traces exhibited anti-correlated fluctuations in the donor and acceptor fluorescence channels, indicative of conformational dynamics on the second time-scale (**Figure S6p-q**). Rap1-dependent chromatin opening for *S2*, but not for *NS*, was associated by an increase in the subset of traces exhibiting such conformational fluctuations (31-37%, **Figure 5i**). This directly indicates that Rap1 samples compact chromatin, and invades chromatin structure, most probably by exploiting intrinsic chromatin fiber dynamics. Once bound, local higher-order structure is disrupted by the pTF, thereby enabling chromatin access for subsequent factors.

Rap1 collaborates with RSC to displace promoter nucleosomes

Taken together, our biophysical analyses show that Rap1 increases accessibility within compact chromatin fibers but does not, by itself, shift or evict bound nucleosomes. Moreover, Rap1 exhibits short residence times on nucleosomal DNA, but is much more stably bound when nucleosomes are removed. The amount of stably-bound Rap1 can be assessed by incubating nucleosomes (containing binding sites *S1* and *S2*) with Rap1 for increasing amounts of time (0 – 90 min) at 30 °C, followed by addition of an excess of competitor plasmid that acts as a sink for all dynamically bound proteins. Following this protocol, no Rap1-bound nucleosomes were detected by native PAGE (**Figure 6a**).

Thus, another factor is required to enable Rap1-dependent clearing of promoters and the establishment of stably-bound Rap1, as observed *in vivo*. In yeast, the RSC complex is involved in the formation and maintenance of nucleosome-free regions within promoters (Badis et al., 2008; Brahma and Henikoff, 2018; Cairns et al., 1996; Hartley and Madhani, 2009; Kubik et al., 2015; Kubik et al., 2018; Ng et al., 2002; Parnell et al., 2008), and plays an important role in the organization of ribosomal

protein gene promoters (Kubik et al., 2015; Kubik et al., 2018). We therefore hypothesized that a remodeler such as RSC could collaborate with Rap1 to expose binding sites and enable stable TF binding.

We used purified RSC complex (Kurat et al., 2017) to perform remodeling assays (Clapier et al., 2016; Lorch et al., 2006) (**Figure 6b**). In the absence of Rap1, RSC slid nucleosomes from their central to a peripheral DNA position (**Figure 6c** and **Figure S7a-b**). When performing these experiments in the presence of Rap1, the repositioned nucleosomes were stably bound by Rap1, as judged by the disappearance of the nucleosomal band (**Figure 6d**, quantified in **Fig. 6e**) as well as the appearance of a new species corresponding to a Rap1-nucleosome complex. These results thus show that nucleosomes remodeled by RSC provide a stable binding environment for Rap1.

Intriguingly, when RSC remodeling and Rap1 binding were performed sequentially, Rap1 nucleosome binding was reduced (**Figure S7e**). This indicated that Rap1 might collaborate with RSC to displace the nucleosome, e.g. by biasing the directionality of the remodeling reaction. We thus performed RSC remodeling experiments (with our without Rap1) on both 601-based (*S1S2*) or *RPL30* nucleosomes, and mapped nucleosome positioning using MNase-seq.

In the absence of Rap1, nucleosomes based on 601 DNA (initially positioned in the DNA center) were primarily shifted by RSC to the DNA end distal to the Rap1 binding sites (**Figure 6f**). In contrast, RSC shifted *RPL30* nucleosomes preferentially towards the Rap1 sites (**Figure 6g**). Such sequence-dependent remodeling by RSC has been described before and is imparted by Rsc3 binding motifs (i.e. variants of CGCG), of which several exist within the 601 sequence, and poly-A tracts, which are present within *RPL30* (Badis et al., 2008; Krietenstein et al., 2016; Kubik et al., 2015; Kubik et al., 2018).

Performing remodeling reactions in the presence of Rap1 altered the nucleosome distributions. In the 601 context, Rap1 could stably bind DNA which was liberated by RSC, and further reduce the nucleosome footprint overlapping with S1 and S2 (**Figure 6f**). In *RPL30* nucleosomes, Rap1 showed a more pronounced effect, reducing RSC-catalyzed nucleosome encroachment over its binding

motifs (**Figure 6g**). Together, these experiments show that Rap1 can bias RSC remodeling, resulting in the clearance of nucleosomes from promoter sequences.

We finally analyzed if such Rap1-coupled dynamic nucleosome repositioning can be observed in living yeast. We generated a yeast strain carrying a reporter plasmid bearing the *RPL30* promoter. Nucleosome positioning on this test promoter was probed by MNase treatment followed by fragment mapping using qPCR (Knight et al., 2014). If at least one functional Rap1 binding motif was present, Rap1 was stably bound, the -1 promoter nucleosome was displaced (**Figure 6h**) and the reporter gene was expressed (**Figure S7g-k**). In contrast, if both Rap1 binding sites were mutated, a nucleosome residing in the NDR was detected and reporter gene expression was abolished (**Figure 6h** and **Figure S7k**). Interestingly, when Rap1 was depleted by an "anchor-away" approach (Haruki et al., 2008; Kubik et al., 2015), the -1 nucleosome was restored for all promoters within 1 h (**Figure 6d**). Subsequent re-induction of Rap1 finally led to rapid nucleosome displacement (< 2h, **Figure 6d**). Together, this demonstrates that Rap1 plays a central role in dynamically altering the local chromatin environment and determining the fate of bound nucleosomes.

DISCUSSION

Elucidating the mechanism of pTF chromatin invasion and remodeling is important for a detailed understanding of gene regulation dynamics. Here, we directly observed the chromatin invasion process of an essential yeast pTF, Rap1, using highly defined reconstituted chromatin systems. The experiments enabled us to draw the following main conclusions. First, Rap1 can bind to both nucleosomes and compact chromatin fibers, but its local dwell times are reduced by higher-level chromatin organization. In contrast, for the binding sites that we probed, target search kinetics driven through nonspecific DNA interactions were not affected by chromatin structure.

Second, we found that Rap1 can access its binding sites *S1* and *S2* without altering the structure of the target nucleosome, but, interestingly, chromatin fiber structure is opened. Stacking interactions between neighboring nucleosomes are disrupted by Rap1, which in turn increases local access.

Third, in controlled *in vitro* experiments we showed that while Rap1 can bind nucleosomes dynamically, stable binding requires collaboration with the RSC remodeler. This conclusion is supported by observations in live yeast cells, where nucleosomes directly targeted by Rap1 are dynamically removed. Together, these data provide a comprehensive view into how the yeast pTF Rap1 locally remodels the chromatin landscape, sculpting a nucleosome-depleted region. In the following, we shall discuss several aspects of our results in the context of the current understanding of pTF function within chromatin.

Multimodal DNA interactions guide Rap1 nucleosome invasion

Several features enable Rap1 to rapidly sample the chromatin landscape and bind to nucleosomal DNA. First the Rap1 DBD is embedded in flanking basic regions which in other TFs have been shown to enable nonspecific DNA binding (Raccaud et al., 2019; Raccaud and Suter, 2018). In our single-molecule studies, we observed frequent short-lived interactions, directly revealing the search process driven by nonspecific DNA contacts within chromatin. Second, Rap1 binds to consensus sequences with very high affinity, ranging in K_d from low pM (e.g. in telomeric motifs (Vignais et al., 1990)) to low nM for various binding motifs (Williams et al., 2010). We observed residence times on the minute to hour time-scale on naked DNA. Third, the Rap1 dual Myb-domains do not completely envelop the target DNA when bound (Konig et al., 1998). Together, this allows Rap1 chromatin binding with similar on-rates as compared to naked DNA and does not require unwrapping of nucleosomal DNA. In contrast, we found that Rap1 residence times on nucleosomes were reduced, albeit not nearly as much as for other TFs (Luo et al., 2014), and that they were dependent on both the nature of the target site and the rotational positioning of the sites on the nucleosome. The reduction in dwell times most probably arises from a combination of partial binding site occlusion and from the highly bent DNA structure on the nucleosome, both known mechanisms that affect TF affinity and sequence specificity (Zhu et al., 2018). Still, due to the flexibility of the Rap1 DBD to engage nucleosomal DNA Rap1 still shows significant chromatin binding, consistent with its role as a pioneer factor. This binding mechanism is similar to

mechanisms observed for mammalian pluripotency factors, such as Sox2 (Soufi et al., 2015), which also bind partial DNA motifs without requiring nucleosome unwrapping. In contrast, two other budding yeast pTFs, Reb1 and Cbf1, have been shown to access nucleosomal DNA by partial nucleosome unwrapping (Donovan et al., 2019). Interestingly, both Reb1 and Cbf1 compensate a reduction in on-rate by increased residence times on nucleosomal substrates. In yet another interaction mode, the mammalian pTF FoxA contains a core-histone binding motif (Cirillo et al., 2002) as well as a DNA-binding domain with similarities to the linker histone H1 (Clark et al., 1993; Iwafuchi-Doi et al., 2016). These motifs thus provide additional stability on chromatin substrates (Cirillo and Zaret, 1999) and open chromatin by linker-histone displacement. Similarly, the related factor FoxO1 can bind to nucleosomes and open linker-histone compacted chromatin (Hatta and Cirillo, 2007). Thus, multiple mechanisms have evolved that allow different pTFs to engage chromatin.

Rap1 passively alters local higher-order chromatin structure

Higher-order chromatin structure reduces Rap1 dwell times but does not preclude binding. Chromatin fibers are conformationally heterogeneous, as exemplified by structural studies (Ekundayo et al., 2017; Garcia-Saez et al., 2018; Routh et al., 2008) or crosslinking experiments (Grigoryev et al., 2009). We and others have previously shown that chromatin fiber contacts are highly dynamic (Kilic et al., 2018b; Li et al., 2016; Poirier et al., 2009). Importantly, the basic units of chromatin organization, tetranucleosome units, exhibit dynamics on a millisecond timescale (Kilic et al., 2018b). This exposes all internal DNA sites over time, yielding opportunities for protein factors to gain access. Here, our data suggest that such local conformational fluctuations enable Rap1, which is retained on chromatin through nonspecific DNA interactions, to access its target sites.

Early experiments based on endonuclease digestion of chromatin fibers indicated that pTFs can increase local chromatin access (Cirillo et al., 2002). Here, we directly observe chromatin fiber structure as a function of pTF invasion using smFRET between neighboring nucleosomes. This provides a molecular view of pTF function, as we could directly observe Rap1 opening local chromatin fiber

structure. Mechanistically, our results suggest that bound Rap1 reduces or blocks the reformation of a closed tetranucleosome unit, as exhibited by the reduction in the high-FRET (HF) state. This not only increases the accessibility for other TFs but also enables binding of remodeling factors that establish a nucleosome-depleted region at promoters.

RSC is required for NDR generation and stable Rap1 binding

Extended NDRs are a prominent feature of active yeast promoters, and Rap1 is a key driver of nucleosome displacement (Ganapathi et al., 2011; Knight et al., 2014; Yu et al., 2001). Chromatin opening *in vivo* has been shown to require the Rap1 DNA binding domain (Yu et al., 2001), but is not reliant on other TFs also found at Rap1-regulated promoters (Ganapathi et al., 2011). However, in our studies we found that Rap1, by itself, is not sufficient to clear a promoter region of nucleosomes. Remodeling factors play a key role in promoter organization (Yen et al., 2012), and have been shown to be important for the activity of multiple pTFs, for example Oct4 or GATA3, which both rely on BRG1 (King and Klose, 2017; Takaku et al., 2016) or INO80 (Wang et al., 2014). Moreover, the synthetic TF Gal4-VP16 was shown to recruit SWI/SNF to open chromatin (Gutierrez et al., 2007).

Here, we show that the yeast remodeling complex RSC displaces nucleosomes and therefore enables stable Rap1 binding and NDR formation. For the *RPL30* promoter, mapping experiments in yeast showed that NDR formation is dependent on both RSC and Rap1, with the latter factor dominating (Kubik et al., 2018). Moreover, the presence of RSC at the RPL30 promoter is influenced by Rap1, further indicating a collaborative function (Kubik et al., 2018). In contrast to mammalian examples that indicate direct remodeler recruitment (King and Klose, 2017), no direct interaction between RSC and Rap1 is described to date. However, RSC might be recruited indirectly or as a result of increased chromatin accessibility upon Rap1 binding.

The directionality of RSC remodeling is controlled by DNA sequence, in particular by poly-dA tracts and GC-rich motifs (Badis et al., 2008; Krietenstein et al., 2016; Kubik et al., 2018). We found however that Rap1 can modulate DNA sequence-directed RSC activity and limit RSC-dependent

encroachment of nucleosomes onto its binding sites. This allows Rap1 to bias the direction of RSC remodeling and to stabilize an open NDR. An attractive mechanistic model for this observation is that Rap1 may act as a "backstop" for RSC activity (**Figure 7**).

The positioning of the Rap1 binding sites relative to the nucleosome dyad might play an important role in determining remodeling direction. Sliding nucleosomes over the Rap1 binding sites might be more energetically disfavored than moving them in the opposite direction. Indeed, this model is supported by nucleosome positioning data for *RPL30* and related yeast promoters (**Figure S7I**) (Kubik et al., 2018). Moreover, RSC- and Rap1-bound remodeling intermediates may provide an explanation for the observation of MNase sensitive fragile nucleosomes at Rap1 bound promoters (Brahma and Henikoff, 2018; Kubik et al., 2015). Finally, upon displacing promoter nucleosomes, Rap1 bound to free DNA sites is no longer impaired by chromatin structure, which results in the long residence times observed for specifically bound Rap1 *in vivo* (Lickwar et al., 2012). Together, our studies thus provide a mechanistic model of how Rap1 accesses chromatin and establishes an active promoter conformation (**Figure 7**).

AUTHOR CONTRIBUTIONS

M.M., B.F., S.K. and D.S. conceived initial experiments. M.M. performed smTIRF and ensemble FRET experiments. A.-M.C. performed smFRET experiments. S.K., S.Z. and D.S. performed yeast experiments. M.M. and R.H. performed remodeling experiments. M.M. and S.Z. performed MNase-seq analysis of remodeling experiments. S.Z. analyzed sequencing data. A.-M.C. and I.B. synthesized dual-labeled chromatin fibers. A.M.S. and M.M. purified Rap1. C.F.K. purified RSC complex and assisted in remodeling experiment. B.F. coordinated the project. All authors were involved in data analysis and interpretation. All authors wrote the manuscript.

ACKNOWLEDGEMENTS

We thank the Swiss National Science foundation (SNSF, grant 31003A_173169 to B.F. and grant 31003A 170153 to D.S.), the NCCR Chemical Biology, EPFL and the Republic and Canton of Geneva for funding. We thank Luke Laevis (Janelia Research Campus) for Halo-JF-549. We thank Louise C. Bryan and Sinan Kilic for human histone octamers.

DECLARATION OF INTERESTS

The authors declare no conflict of interest.

FIGURES

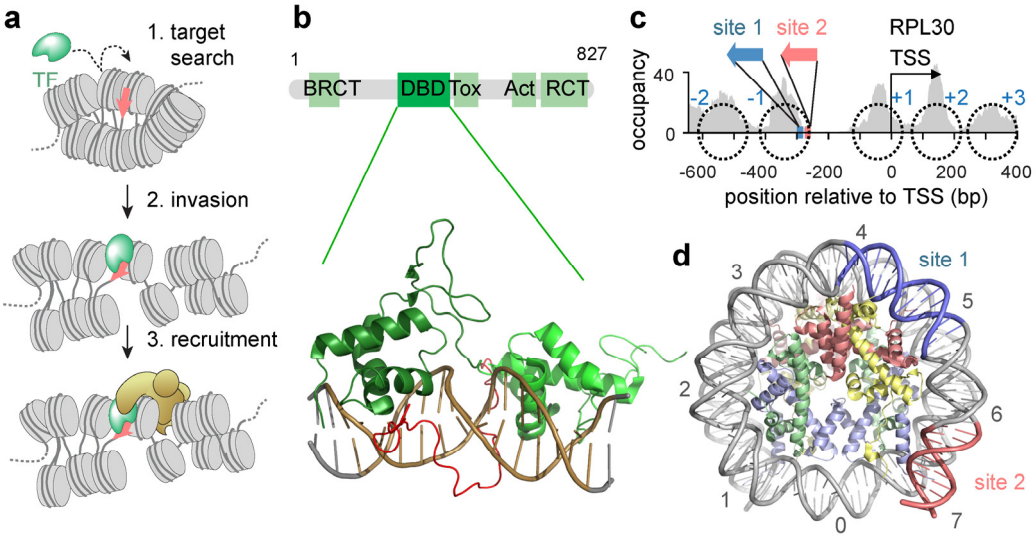

Figure 1: Rap1 as a pioneer factor in budding yeast. a) Scheme of pTF function: After a target search (1) for its cognate binding site, the pTF invades compact chromatin structure (2), followed by local chromatin opening and recruitment of the transcription machinery (3). **b**) Domain organization of budding yeast Rap1 (above) and X-ray crystal structure of Rap1 in complex with its cognate DNA motif (PDB code 3ukg, (Matot et al., 2012)). Rap1 is constituted of several regions including a BRCA 1 C-Terminus (BRCT), DNA Binding Domain (DBD), Toxicity region (Tox), Transcription Activation domain (Act) and the Rap1 C-Terminus (RCT). **c**) The organization of the *RPL30* promoter. Grey: MNase-seq profile (Rap1 depleted by anchor-away) (Kubik et al., 2015) reveals nucleosome positions in the absence of Rap1 (black dotted circles). Plotted is nucleosome occupancy reads, normalized to 10^7 total reads. The Rap1 binding site 1 (*S1*, high affinity) and site 2 (*S2*, medium affinity) fall on the -1 nucleosome. **d**) Promoter -1 nucleosome, showing Rap1 binding sites *S1* and *S2* mapped on the DNA (PDB code 1AOI, (Luger et al., 1997)). The numbers indicate super helical locations (SHL) of the nucleosomal DNA.

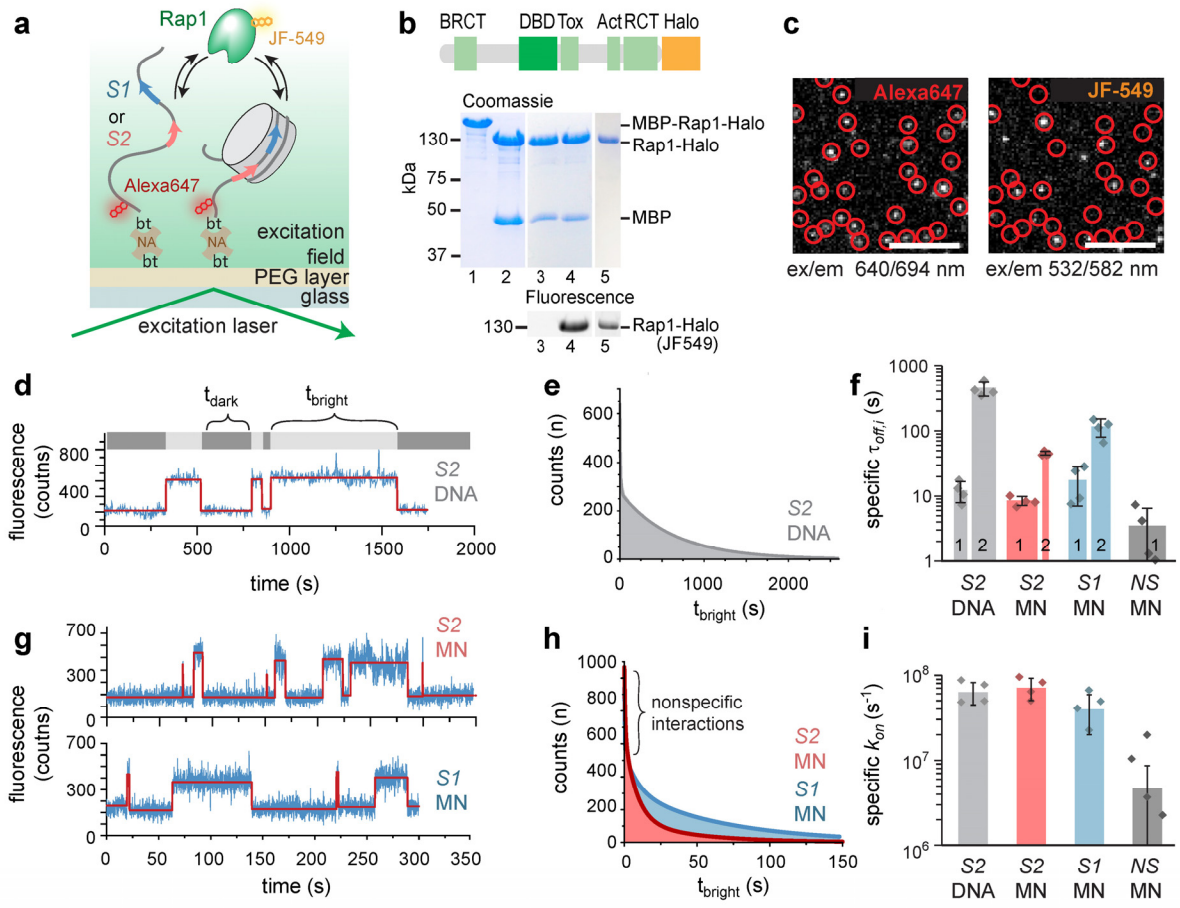

Figure 2: Rap1 recognizes target sites within nucleosomal DNA. a) Schematic view of the smTIRFM experiment, probing Rap1 binding to immobilized DNA or nucleosomes (bt-NA: biotin-neutravidin), containing either *S1* or *S2* and labeled with AlexaFluor 647. **b**) Expression of JF-549 labeled Rap1, using Halo-tag. Lanes: 1. Purified MBP-Rap1-Halo construct; 2. MBP cleaved; 3. Before JF-549 labeling; 4. After JF-549 labeling; 5. Purified, labeled Rap1 construct. **c**) Representative smTIRF images showing nucleosome positions in the far red channel (left, red-circles) and Rap1 interaction dynamics in the green-orange channel (right). Scale bar: 5 µm; ex, excitation wavelength; em, emission wavelength. **d**) Representative fluorescence time trace of Rap1 binding events to *S2* containing free DNA, detected by JF-549 emission. The trace is fitted by step function (red) and t_{dark} and t_{bright} were determined by a thresholding algorithm. **e**) Cumulative histogram of Rap1 binding intervals (t_{bright}) on *S2* DNA fitted by a 2-exponential function $y = \sum_{i=1}^{2} A_i \exp(-t/\tau_{off,i})$ (solid line). For all fit results, see **Table S1**. **f**) Specific dissociation time constants ($\tau_{off,i}$ > 1 s) of Rap1 for *S2* DNA, *S1* and *S2* containing mononucleosomes (MN) or nucleosomes lacking a binding site (601), uncorrected for dye photobleaching. The width of the bars indicate the percentage of events associated with the indicated time constants (i.e. amplitudes A_i of the multi-exponential fits shown in **e**,**h**). N = 4-5, error bars: s.d. **g**) Representative fluorescence time trace of Rap1 binding events to *S1* (bottom) and *S2* (top) containing MNs. The data was analyzed as in **d**. **h**) Cumulative histogram of Rap1 binding intervals (t_{bright}) on *S1* and *S2* containing MNs fitted by a 3-exponential function $y = \sum_{i=0}^{2} A_i \exp(-t/\tau_{off,i})$ (solid line). **i**) Specific on-rates ($k_{on} = 1/\tau_{on}$), for all species obtained from a single-exponential fit to cumulative histograms of t_{dark} values, and corrected for the contribution from non-specific interactions (**Supplementary information**).

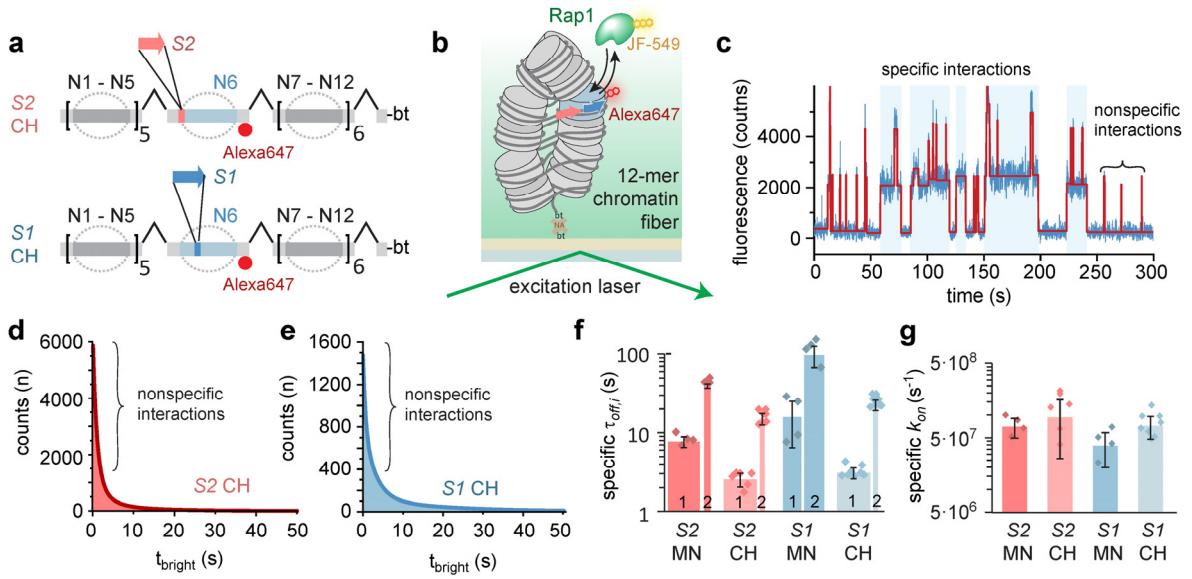

Figure 3: Chromatin higher-order structure reduces Rap1 dwell time. a) Schematic view of DNA preparation to introduce Rap1 target sites *S1* and *S2* into the central nucleosomes (N6) of a chromatin fiber (CH). **b**) Scheme of the smTIRFM experiment to measure Rap1 binding kinetics in a chromatin fiber context. **c**) Representative fluorescence time trace of Rap1 binding events to *S1*-containing chromatin arrays. The trace is fitted by a step function (red) and t_{dark} and t_{bright} were determined by a thresholding algorithm. **d**) Cumulative histogram of Rap1 binding intervals (t_{bright}) to chromatin fibers, containing *S1* fitted by a 3-exponential function (solid line). For all fit results, see **Table S1**. **e**) Cumulative histogram of Rap1 binding to chromatin arrays, containing *S2* fitted by a 3-exponential function (solid line). **f**) Specific binding time constants ($\tau_{off,i}$ > 1 s) of Rap1 for S1 in a nucleosome (MN) vs. chromatin fiber (CH) and S2 MN vs CH. The width of the bars indicate the percentage of events associated with the indicated time constants (i.e. amplitudes A_i of the multi-exponential fits shown in **d**,**e**). N = 4-5, error bars: s.d. **g**) Specific on-rates ($k_{on} = 1/\tau_{on}$), for mononucleosomes (MN) and chromatin fibers (CH) containing *S1* and *S2*, obtained from a single-exponential fit to cumulative histograms of t_{dark} values, and corrected for the contribution from non-specific interactions (**Supplementary information**).

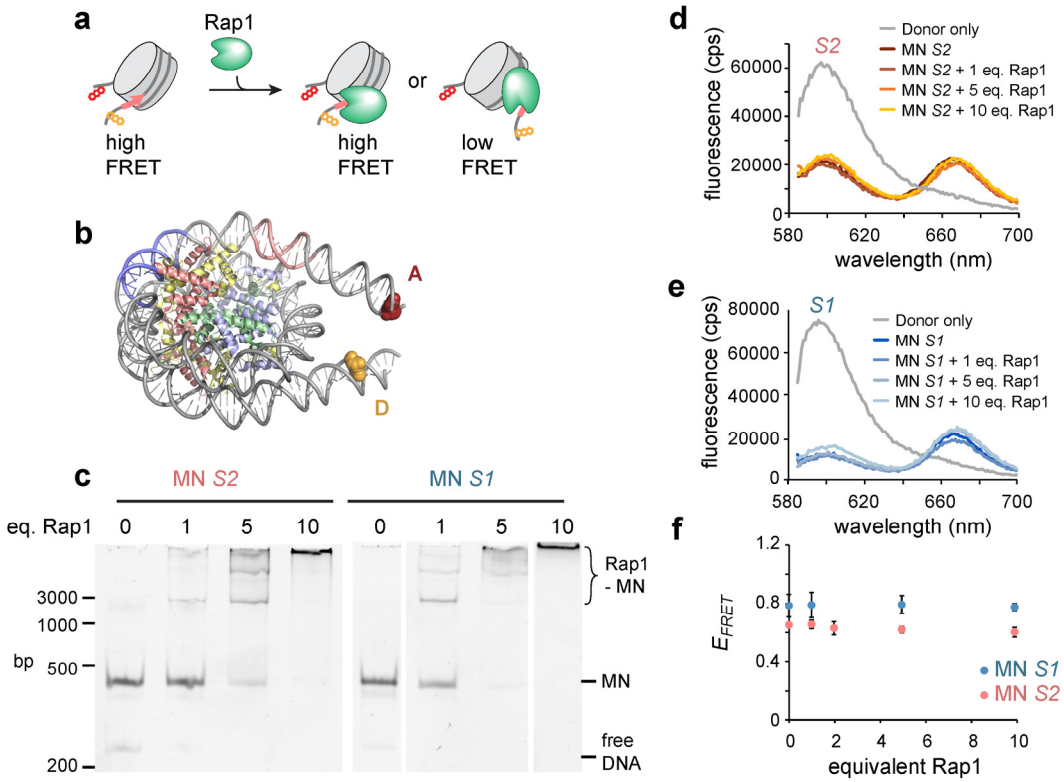

Figure 4: Rap1 does not open nucleosome structure. **a**) Scheme of a FRET approach to probe nucleosome structure as a function of bound Rap1. **b**) Nucleosome structure (PDB code 1AOI) showing attachment points of FRET probes. **c**) EMSA showing Rap1 binding to *S1* and *S2* nucleosomes at indicated concentration equivalents (eq.). **d**) Fluorescence spectra for *S2* nucleosome in complex with indicated equivalents of Rap1. **e**) Fluorescence spectra for *S1* nucleosome in complex with indicated equivalents of Rap1. **f**) FRET efficiency calculated for *S2* and *S1* nucleosomes as a function of equivalents added Rap1. Error bars: s.d., n = 2.

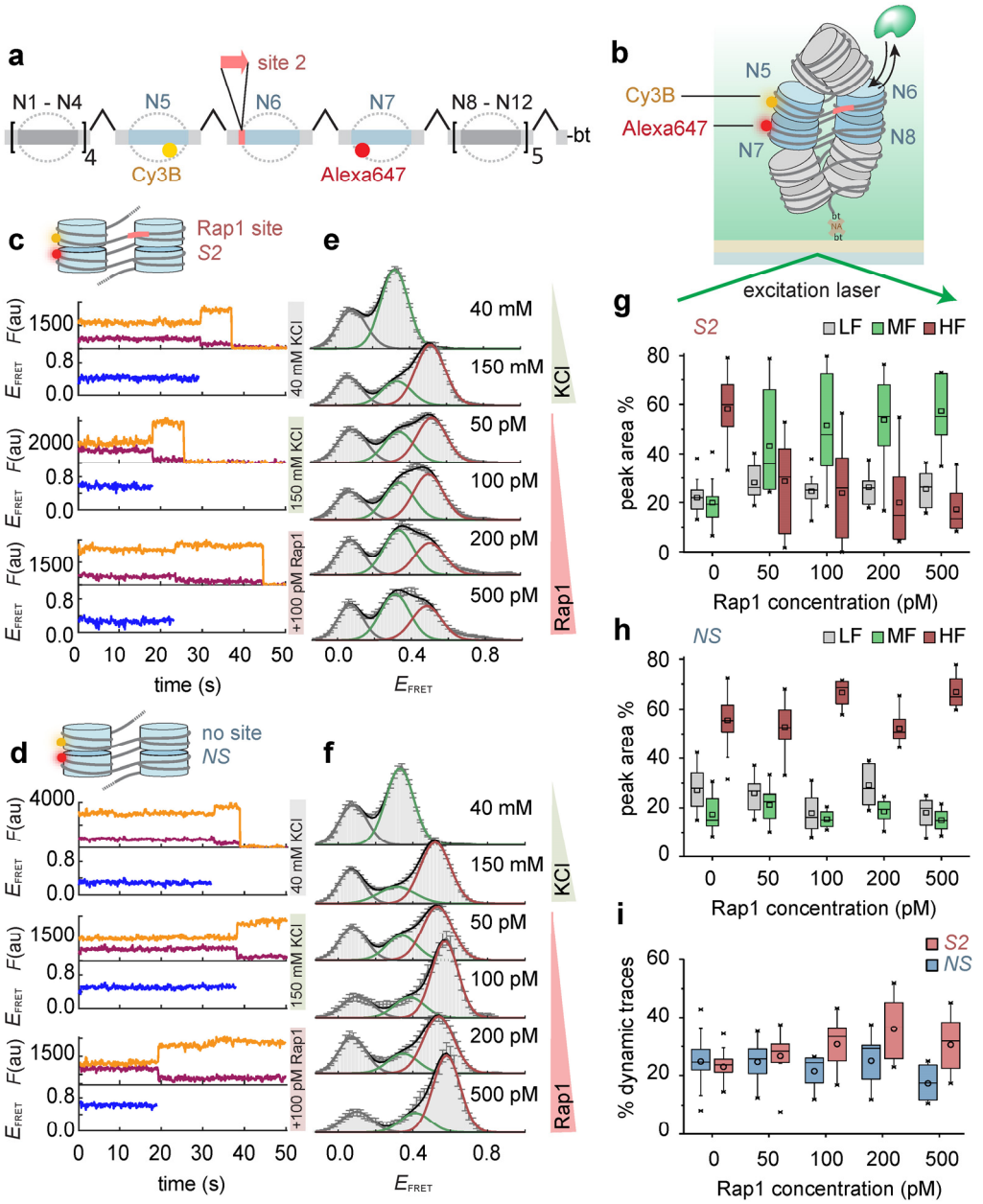

Figure 5: Chromatin remodeling induced by Rap1 invasion as observed by smFRET. a) Scheme of chromatin DNA assembly to introduce a Rap1 site at nucleosome N6, as well as a FRET donor (Cy3B, yellow) and acceptor (Alexa647, red) at nucleosomes N5 and N7. **b**) Scheme of a smFRET-TIRF experiment. **c**) Individual kinetic traces of donor (orange) and acceptor (red) fluorescence emission, and FRET efficiency (E_{FRET}, blue) for chromatin fibers containing *S2* at the indicated KCl and Rap1 concentrations. All Rap1 experiments were performed at 150 mM KCl. **d**) Similar to **c**) but for chromatin lacking Rap1 binding sites (*NS*). **e**) Histograms of E_{FRET} of *S2*-containing chromatin fibers at the indicated KCl and Rap1 concentrations. All Rap1 experiments were performed at 150 mM KCl. Histograms were fitted by Gaussian functions, revealing a low-FRET (LF, grey), medium-FRET (MF, green) and high-FRET (HF, red) population. Error bars are s.e.m., for the number of traces and parameters of Gaussian fits see **Tables S5** & **S6**. **f**) Similar to **e**) but for chromatin lacking Rap1 binding sites (*NS*). **g**) Percentage of each FRET sub-population, low-FRET (LF), medium-FRET (MF) and high-FRET (HF) for chromatin containing *S2*. Box: 25-75 percentiles, whiskers: outliers (factor 1.5), line: median, open symbol: mean. For number of experiments see **Table S6**. **h**) Similar to **g**) but for chromatin lacking Rap1 binding sites (*NS*). **i**) Percentage of dynamic traces for *S2* and *NS* chromatin. Box: similar to **h**). For the identification of dynamic traces see **Supplementary information**).

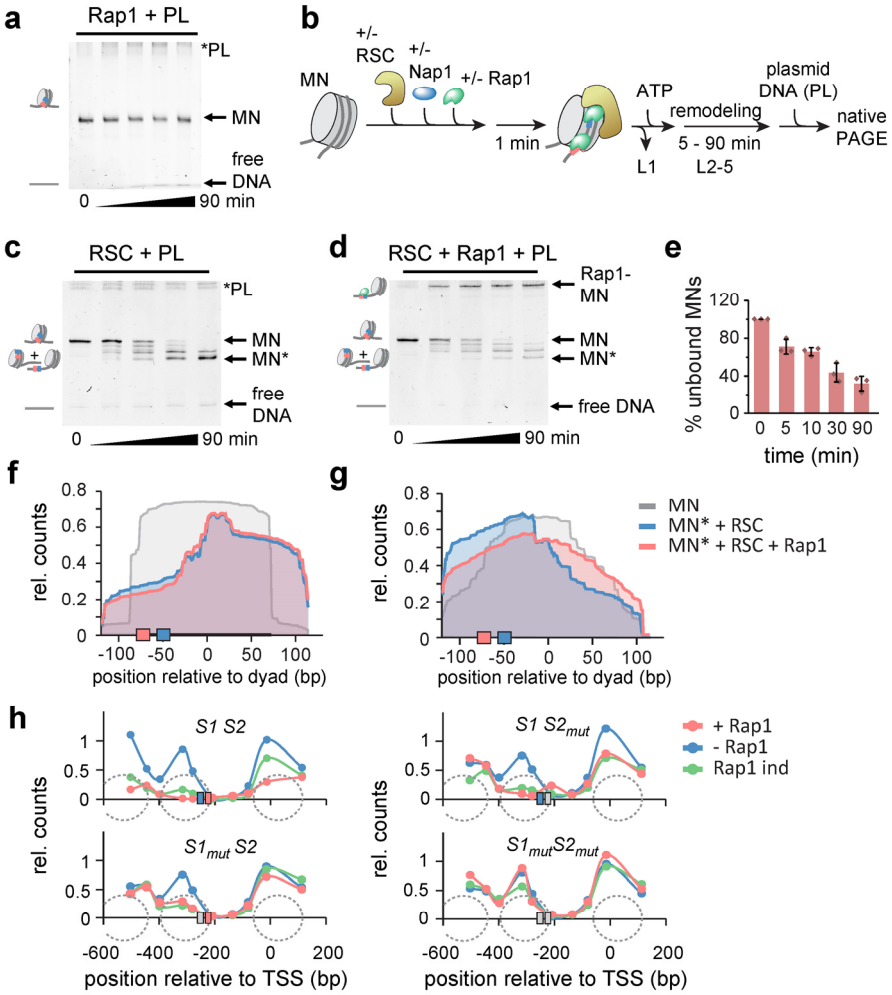

Figure 6: RSC enables stable Rap1 binding by exposing binding sites. a) Native PAGE analysis of Rap1 binding for indicated times followed by incubation with competitor plasmid DNA (PL). L1, L2-L5: Lanes in panels **a**) and **c,d**). **b**) Scheme of RSC remodeling assay. Note that Nap1 is not strictly required in these experiments (**Figure S6c**). **c**) Native PAGE analysis of remodeling assays; MN*: remodeled mononucleosome. **d**) Native PAGE analysis of remodeling assays in the presence of 10 eq. of Rap1. **e**) Integrated unbound nucleosome bands from **d**) (n = 3, error bars s.d.). **f**) MNase-seq results from RSC remodeling assays for 601 nucleosomes (P3_S1S2). Grey: nucleosome start position, blue: RSC remodeling for 90 min in absence of Rap1, red: RSC remodeling for 90 min in presence of 10 eq. Rap1. Shown are reads normalized to number of total reads. **g**) Same as in **f**) but for *RPL30* nucleosomes (P3_RPL30). **h**) Effect of Rap1 binding on nucleosome stability at the *RPL30* promoter in yeast. Nucleosome positions were determined using qPCR after MNase digestion of chromatin. Promoters analyzed contained both Rap1 binding sites (*S1S2*), *S1* mutated ($S1_{mut}S2$), *S2* mutated ($S1S2_{mut}$) or both binding sites mutated ($S1_{mut}S2_{mut}$). Data shown are for cells where Rap1 is present (Rap1+, red), Rap1 has been depleted from the nucleus for 1 h by anchor-away (Rap1-, blue), and where Rap1 has been re-introduced for 2h following depletion by expressing a *RAP1* construct from an inducible promoter (Rap1 ind, green).

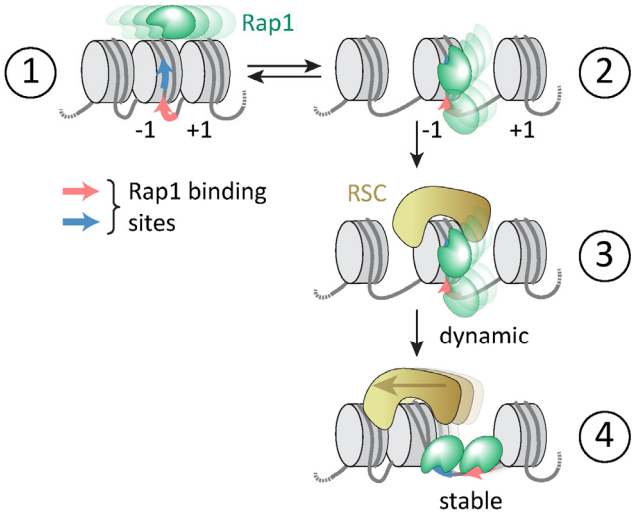

Figure 7: A dynamic model for Rap1 mediated promoter chromatin remodeling. Rap1 searches chromatin (step 1) and its dynamic binding (2-25 s) to a promoter site results in local chromatin opening (step 2), where Rap1 remains dynamically bound. RSC mediated nucleosome sliding opens the NDR and exposes the DNA containing Rap1 binding sites (step 3). The fully exposed binding sites allow stable Rap1 binding (step 4) with long residence times (compare free DNA τ_{res} > 450 s), and prevent further nucleosome encroachment.

REFERENCES

Adams, C.C., and Workman, J.L. (1995). Binding of disparate transcriptional activators to nucleosomal DNA is inherently cooperative. Mol Cell Biol *15*, 1405-1421.

Allahverdi, A., Chen, Q., Korolev, N., and Nordenskiold, L. (2015). Chromatin compaction under mixed salt conditions: opposite effects of sodium and potassium ions on nucleosome array folding. Sci Rep *5*, 8512.

Badis, G., Chan, E.T., van Bakel, H., Pena-Castillo, L., Tillo, D., Tsui, K., Carlson, C.D., Gossett, A.J., Hasinoff, M.J., Warren, C.L*., et al.* (2008). A library of yeast transcription factor motifs reveals a widespread function for Rsc3 in targeting nucleosome exclusion at promoters. Mol Cell *32*, 878-887.

Brahma, S., and Henikoff, S. (2018). RSC-Associated Subnucleosomes Define MNase-Sensitive Promoters in Yeast. Mol Cell.

Cairns, B.R., Lorch, Y., Li, Y., Zhang, M., Lacomis, L., Erdjument-Bromage, H., Tempst, P., Du, J., Laurent, B., and Kornberg, R.D. (1996). RSC, an essential, abundant chromatin-remodeling complex. Cell *87*, 1249-1260.

Challal, D., Barucco, M., Kubik, S., Feuerbach, F., Candelli, T., Geoffroy, H., Benaksas, C., Shore, D., and Libri, D. (2018). General Regulatory Factors Control the Fidelity of Transcription by Restricting Non-coding and Ectopic Initiation. Mol Cell *72*, 955-969 e957.

Chereji, R.V., Ocampo, J., and Clark, D.J. (2017). MNase-Sensitive Complexes in Yeast: Nucleosomes and Non-histone Barriers. Mol Cell *65*, 565-577 e563.

Chung, S.H., and Kennedy, R.A. (1991). Forward-backward non-linear filtering technique for extracting small biological signals from noise. Journal of neuroscience methods *40*, 71-86.

Cirillo, L.A., Lin, F.R., Cuesta, I., Friedman, D., Jarnik, M., and Zaret, K.S. (2002). Opening of compacted chromatin by early developmental transcription factors HNF3 (FoxA) and GATA-4. Mol Cell *9*, 279-289.

Cirillo, L.A., and Zaret, K.S. (1999). An early developmental transcription factor complex that is more stable on nucleosome core particles than on free DNA. Mol Cell *4*, 961-969.

Clapier, C.R., Kasten, M.M., Parnell, T.J., Viswanathan, R., Szerlong, H., Sirinakis, G., Zhang, Y., and Cairns, B.R. (2016). Regulation of DNA Translocation Efficiency within the Chromatin Remodeler RSC/Sth1 Potentiates Nucleosome Sliding and Ejection. Mol Cell *62*, 453-461.

Clark, K.L., Halay, E.D., Lai, E.S., and Burley, S.K. (1993). Co-Crystal Structure of the Hnf-3/Fork Head DNA-Recognition Motif Resembles Histone-H5. Nature *364*, 412-420.

Cuvier, O., and Fierz, B. (2017). Dynamic chromatin technologies: from individual molecules to epigenomic regulation in cells. Nat Rev Genet.

Donovan, B.T., Chen, H., Jipa, C., Bai, L., and Poirier, M.G. (2019). Dissociation rate compensation mechanism for budding yeast pioneer transcription factors. eLife *8*.

Dorigo, B., Schalch, T., Bystricky, K., and Richmond, T.J. (2003). Chromatin fiber folding: requirement for the histone H4 N-terminal tail. J Mol Biol *327*, 85-96.

Dyer, P.N., Edayathumangalam, R.S., White, C.L., Bao, Y., Chakravarthy, S., Muthurajan, U.M., and Luger, K. (2004). Reconstitution of nucleosome core particles from recombinant histones and DNA. Methods Enzymol *375*, 23-44.

Ekundayo, B., Richmond, T.J., and Schalch, T. (2017). Capturing Structural Heterogeneity in Chromatin Fibers. J Mol Biol *429*, 3031-3042.

Fakhouri, T.H., Stevenson, J., Chisholm, A.D., and Mango, S.E. (2010). Dynamic chromatin organization during foregut development mediated by the organ selector gene PHA-4/FoxA. PLoS Genet *6*.

Feldmann, E.A., and Galletto, R. (2014). The DNA-binding domain of yeast Rap1 interacts with double-stranded DNA in multiple binding modes. Biochemistry *53*, 7471-7483.

Fierz, B., Chatterjee, C., McGinty, R.K., Bar-Dagan, M., Raleigh, D.P., and Muir, T.W. (2011). Histone H2B ubiquitylation disrupts local and higher-order chromatin compaction. Nat Chem Biol *7*, 113-119.

Ganapathi, M., Palumbo, M.J., Ansari, S.A., He, Q., Tsui, K., Nislow, C., and Morse, R.H. (2011). Extensive role of the general regulatory factors, Abf1 and Rap1, in determining genome-wide chromatin structure in budding yeast. Nucleic Acids Res *39*, 2032-2044.

Garcia-Saez, I., Menoni, H., Boopathi, R., Shukla, M.S., Soueidan, L., Noirclerc-Savoye, M., Le Roy, A., Skoufias, D.A., Bednar, J., Hamiche, A*., et al.* (2018). Structure of an H1-Bound 6-Nucleosome Array Reveals an Untwisted Two-Start Chromatin Fiber Conformation. Mol Cell.

Grigoryev, S.A., Arya, G., Correll, S., Woodcock, C.L., and Schlick, T. (2009). Evidence for heteromorphic chromatin fibers from analysis of nucleosome interactions. Proc Natl Acad Sci USA *106*, 13317-13322.

Grimm, J.B., English, B.P., Chen, J., Slaughter, J.P., Zhang, Z., Revyakin, A., Patel, R., Macklin, J.J., Normanno, D., Singer, R.H*., et al.* (2015). A general method to improve fluorophores for live-cell and single-molecule microscopy. Nat Methods *12*, 244-250, 243 p following 250.

Gutierrez, J.L., Chandy, M., Carrozza, M.J., and Workman, J.L. (2007). Activation domains drive nucleosome eviction by SWI/SNF. EMBO J *26*, 730-740.

Hartley, P.D., and Madhani, H.D. (2009). Mechanisms that specify promoter nucleosome location and identity. Cell *137*, 445-458.

Haruki, H., Nishikawa, J., and Laemmli, U.K. (2008). The anchor-away technique: rapid, conditional establishment of yeast mutant phenotypes. Mol Cell *31*, 925-932.

Hatta, M., and Cirillo, L.A. (2007). Chromatin opening and stable perturbation of core histone:DNA contacts by FoxO1. J Biol Chem *282*, 35583-35593.

Henikoff, J.G., Belsky, J.A., Krassovsky, K., MacAlpine, D.M., and Henikoff, S. (2011). Epigenome characterization at single base-pair resolution. Proc Natl Acad Sci U S A *108*, 18318-18323.

Hsieh, T.H., Weiner, A., Lajoie, B., Dekker, J., Friedman, N., and Rando, O.J. (2015). Mapping Nucleosome Resolution Chromosome Folding in Yeast by Micro-C. Cell *162*, 108-119.

Iwafuchi-Doi, M., Donahue, G., Kakumanu, A., Watts, J.A., Mahony, S., Pugh, B.F., Lee, D., Kaestner, K.H., and Zaret, K.S. (2016). The Pioneer Transcription Factor FoxA Maintains an Accessible Nucleosome Configuration at Enhancers for Tissue-Specific Gene Activation. Mol Cell *62*, 79-91.

Jiang, C., and Pugh, B.F. (2009). Nucleosome positioning and gene regulation: advances through genomics. Nat Rev Genet *10*, 161-172.

Jin, C., Zang, C., Wei, G., Cui, K., Peng, W., Zhao, K., and Felsenfeld, G. (2009). H3.3/H2A.Z double variant-containing nucleosomes mark 'nucleosome-free regions' of active promoters and other regulatory regions. Nat Genet *41*, 941-945.

Kent, N.A., Adams, S., Moorhouse, A., and Paszkiewicz, K. (2011). Chromatin particle spectrum analysis: a method for comparative chromatin structure analysis using paired-end mode next-generation DNA sequencing. Nucleic Acids Res *39*, e26.

Kilic, S., Bachmann, A.L., Bryan, L.C., and Fierz, B. (2015). Multivalency governs HP1alpha association dynamics with the silent chromatin state. Nat Commun *6*, 7313.

Kilic, S., Boichenko, I., Lechner, C.C., and Fierz, B. (2018a). A bi-terminal protein ligation strategy to probe chromatin structure during DNA damage. Chem Sci *9*, 3704-3709

Kilic, S., Felekyan, S., Doroshenko, O., Boichenko, I., Dimura, M., Vardanyan, H., Bryan, L.C., Arya, G., Seidel, C.A.M., and Fierz, B. (2018b). Single-molecule FRET reveals multiscale chromatin dynamics modulated by HP1alpha. Nat Commun *9*, 235.

King, H.W., and Klose, R.J. (2017). The pioneer factor OCT4 requires the chromatin remodeller BRG1 to support gene regulatory element function in mouse embryonic stem cells. eLife *6*.

Knight, B., Kubik, S., Ghosh, B., Bruzzone, M.J., Geertz, M., Martin, V., Denervaud, N., Jacquet, P., Ozkan, B., Rougemont, J.*, et al.* (2014). Two distinct promoter architectures centered on dynamic nucleosomes control ribosomal protein gene transcription. Genes Dev *28*, 1695-1709.

Koerber, R.T., Rhee, H.S., Jiang, C., and Pugh, B.F. (2009). Interaction of transcriptional regulators with specific nucleosomes across the Saccharomyces genome. Molecular cell *35*, 889-902.

Konig, P., Fairall, L., and Rhodes, D. (1998). Sequence-specific DNA recognition by the myb-like domain of the human telomere binding protein TRF1: a model for the protein-DNA complex. Nucleic Acids Res *26*, 1731-1740.

Krietenstein, N., Wal, M., Watanabe, S., Park, B., Peterson, C.L., Pugh, B.F., and Korber, P. (2016). Genomic Nucleosome Organization Reconstituted with Pure Proteins. Cell *167*, 709-721 e712.

Kubik, S., Bruzzone, M.J., Albert, B., and Shore, D. (2017). A Reply to "MNase-Sensitive Complexes in Yeast: Nucleosomes and Non-histone Barriers," by Chereji et al. Mol Cell *65*, 578-580.

Kubik, S., Bruzzone, M.J., Jacquet, P., Falcone, J.L., Rougemont, J., and Shore, D. (2015). Nucleosome Stability Distinguishes Two Different Promoter Types at All Protein-Coding Genes in Yeast. Mol Cell *60*, 422-434.

Kubik, S., O'Duibhir, E., de Jonge, W.J., Mattarocci, S., Albert, B., Falcone, J.L., Bruzzone, M.J., Holstege, F.C.P., and Shore, D. (2018). Sequence-Directed Action of RSC Remodeler and General Regulatory Factors Modulates +1 Nucleosome Position to Facilitate Transcription. Mol Cell *71*, 89-102 e105.

Kurat, C.F., Yeeles, J.T.P., Patel, H., Early, A., and Diffley, J.F.X. (2017). Chromatin Controls DNA Replication Origin Selection, Lagging-Strand Synthesis, and Replication Fork Rates. Mol Cell *65*, 117-130.

Li, G., Levitus, M., Bustamante, C., and Widom, J. (2005). Rapid spontaneous accessibility of nucleosomal DNA. Nat Struct Mol Biol *12*, 46-53.

Li, G., and Widom, J. (2004). Nucleosomes facilitate their own invasion. Nat Struct Mol Biol *11*, 763-769.

Li, W., Chen, P., Yu, J., Dong, L., Liang, D., Feng, J., Yan, J., Wang, P.Y., Li, Q., Zhang, Z.*, et al.* (2016). FACT Remodels the Tetranucleosomal Unit of Chromatin Fibers for Gene Transcription. Mol Cell *64*, 120-133.

Lickwar, C.R., Mueller, F., Hanlon, S.E., McNally, J.G., and Lieb, J.D. (2012). Genome-wide protein-DNA binding dynamics suggest a molecular clutch for transcription factor function. Nature *484*, 251-255.

Lieb, J.D., Liu, X., Botstein, D., and Brown, P.O. (2001). Promoter-specific binding of Rap1 revealed by genome-wide maps of protein-DNA association. Nat Genet *28*, 327-334.

Lorch, Y., Maier-Davis, B., and Kornberg, R.D. (2006). Chromatin remodeling by nucleosome disassembly in vitro. Proc Natl Acad Sci U S A *103*, 3090-3093.

Luger, K., Mader, A.W., Richmond, R.K., Sargent, D.F., and Richmond, T.J. (1997). Crystal structure of the nucleosome core particle at 2.8 A resolution. Nature *389*, 251-260.

Luo, Y., North, J.A., Rose, S.D., and Poirier, M.G. (2014). Nucleosomes accelerate transcription factor dissociation. Nucleic Acids Res *42*, 3017-3027.

Matot, B., Le Bihan, Y.V., Lescasse, R., Perez, J., Miron, S., David, G., Castaing, B., Weber, P., Raynal, B., Zinn-Justin, S.*, et al.* (2012). The orientation of the C-terminal domain of the Saccharomyces cerevisiae Rap1 protein is determined by its binding to DNA. Nucleic Acids Res *40*, 3197-3207.

Mirny, L.A. (2010). Nucleosome-mediated cooperativity between transcription factors. Proc Natl Acad Sci U S A *107*, 22534-22539.

Ng, H.H., Robert, F., Young, R.A., and Struhl, K. (2002). Genome-wide location and regulated recruitment of the RSC nucleosome-remodeling complex. Genes Dev *16*, 806-819.

Parnell, T.J., Huff, J.T., and Cairns, B.R. (2008). RSC regulates nucleosome positioning at Pol II genes and density at Pol III genes. EMBO J *27*, 100-110.

Poirier, M.G., Bussiek, M., Langowski, J., and Widom, J. (2008). Spontaneous access to DNA target sites in folded chromatin fibers. J Mol Biol *379*, 772-786.

Poirier, M.G., Oh, E., Tims, H.S., and Widom, J. (2009). Dynamics and function of compact nucleosome arrays. Nat Struct Mol Biol *16*, 938-944.

Raccaud, M., Friman, E.T., Alber, A.B., Agarwal, H., Deluz, C., Kuhn, T., Gebhardt, J.C.M., and Suter, D.M. (2019). Mitotic chromosome binding predicts transcription factor properties in interphase. Nat Commun *10*, 487.

Raccaud, M., and Suter, D.M. (2018). Transcription factor retention on mitotic chromosomes: regulatory mechanisms and impact on cell fate decisions. FEBS Lett *592*, 878-887.

Rawal, Y., Chereji, R.V., Qiu, H., Ananthakrishnan, S., Govind, C.K., Clark, D.J., and Hinnebusch, A.G. (2018). SWI/SNF and RSC cooperate to reposition and evict promoter nucleosomes at highly expressed genes in yeast. Genes Dev *32*, 695-710.

Risca, V.I., Denny, S.K., Straight, A.F., and Greenleaf, W.J. (2017). Variable chromatin structure revealed by in situ spatially correlated DNA cleavage mapping. Nature *541*, 237-241.

Rossetti, L., Cacchione, S., De Menna, A., Chapman, L., Rhodes, D., and Savino, M. (2001). Specific interactions of the telomeric protein Rap1p with nucleosomal binding sites. J Mol Biol *306*, 903-913.

Routh, A., Sandin, S., and Rhodes, D. (2008). Nucleosome repeat length and linker histone stoichiometry determine chromatin fiber structure. Proc Natl Acad Sci U S A *105*, 8872-8877.

Schalch, T., Duda, S., Sargent, D.F., and Richmond, T.J. (2005). X-ray structure of a tetranucleosome and its implications for the chromatin fibre. Nature *436*, 138-141.

Song, F., Chen, P., Sun, D., Wang, M., Dong, L., Liang, D., Xu, R.M., Zhu, P., and Li, G. (2014). Cryo-EM study of the chromatin fiber reveals a double helix twisted by tetranucleosomal units. Science *344*, 376-380.

Soufi, A., Donahue, G., and Zaret, K.S. (2012). Facilitators and impediments of the pluripotency reprogramming factors' initial engagement with the genome. Cell *151*, 994-1004.

Soufi, A., Garcia, M.F., Jaroszewicz, A., Osman, N., Pellegrini, M., and Zaret, K.S. (2015). Pioneer transcription factors target partial DNA motifs on nucleosomes to initiate reprogramming. Cell *161*, 555-568.

Suto, R.K., Clarkson, M.J., Tremethick, D.J., and Luger, K. (2000). Crystal structure of a nucleosome core particle containing the variant histone H2A.Z. Nat Struct Biol *7*, 1121-1124.

Takaku, M., Grimm, S.A., Shimbo, T., Perera, L., Menafra, R., Stunnenberg, H.G., Archer, T.K., Machida, S., Kurumizaka, H., and Wade, P.A. (2016). GATA3-dependent cellular reprogramming requires activation-domain dependent recruitment of a chromatin remodeler. Genome biology *17*, 36.

Thastrom, A., Lowary, P.T., Widlund, H.R., Cao, H., Kubista, M., and Widom, J. (1999). Sequence motifs and free energies of selected natural and non-natural nucleosome positioning DNA sequences. J Mol Biol *288*, 213-229.

van Bakel, H., Tsui, K., Gebbia, M., Mnaimneh, S., Hughes, T.R., and Nislow, C. (2013). A compendium of nucleosome and transcript profiles reveals determinants of chromatin architecture and transcription. PLoS Genet *9*, e1003479.

Vignais, M.L., Huet, J., Buhler, J.M., and Sentenac, A. (1990). Contacts between the factor TUF and RPG sequences. J Biol Chem *265*, 14669-14674.

Wang, L., Du, Y., Ward, J.M., Shimbo, T., Lackford, B., Zheng, X., Miao, Y.L., Zhou, B., Han, L., Fargo, D.C.*, et al.* (2014). INO80 facilitates pluripotency gene activation in embryonic stem cell self-renewal, reprogramming, and blastocyst development. Cell Stem Cell *14*, 575-591.

Weiner, A., Hughes, A., Yassour, M., Rando, O.J., and Friedman, N. (2010). High-resolution nucleosome mapping reveals transcription-dependent promoter packaging. Genome Res *20*, 90-100.

Wellinger, R.J., and Zakian, V.A. (2012). Everything you ever wanted to know about Saccharomyces cerevisiae telomeres: beginning to end. Genetics *191*, 1073-1105.

Williams, T.L., Levy, D.L., Maki-Yonekura, S., Yonekura, K., and Blackburn, E.H. (2010). Characterization of the yeast telomere nucleoprotein core: Rap1 binds independently to each recognition site. J Biol Chem *285*, 35814-35824.

Wu, A.C.K., Patel, H., Chia, M., Moretto, F., Frith, D., Snijders, A.P., and van Werven, F.J. (2018). Repression of Divergent Noncoding Transcription by a Sequence-Specific Transcription Factor. Mol Cell *72*, 942-954 e947.

Xi, Y., Yao, J., Chen, R., Li, W., and He, X. (2011). Nucleosome fragility reveals novel functional states of chromatin and poises genes for activation. Genome Res *21*, 718-724.

Yan, C., Chen, H., and Bai, L. (2018). Systematic Study of Nucleosome-Displacing Factors in Budding Yeast. Mol Cell *71*, 294-305 e294.

Yen, K., Vinayachandran, V., Batta, K., Koerber, R.T., and Pugh, B.F. (2012). Genome-wide nucleosome specificity and directionality of chromatin remodelers. Cell *149*, 1461-1473.

Yu, L., and Morse, R.H. (1999). Chromatin opening and transactivator potentiation by RAP1 in Saccharomyces cerevisiae. Mol Cell Biol *19*, 5279-5288.

Yu, L., Sabet, N., Chambers, A., and Morse, R.H. (2001). The N-terminal and C-terminal domains of RAP1 are dispensable for chromatin opening and GCN4-mediated HIS4 activation in budding yeast. J Biol Chem *276*, 33257-33264.

Zaret, K.S., and Carroll, J.S. (2011). Pioneer transcription factors: establishing competence for gene expression. Genes Dev *25*, 2227-2241.

Zaret, K.S., and Mango, S.E. (2016). Pioneer transcription factors, chromatin dynamics, and cell fate control. Curr Opin Genet Dev *37*, 76-81.

Zentner, G.E., and Henikoff, S. (2012). Surveying the epigenomic landscape, one base at a time. Genome biology *13*, 250.

Zhu, F., Farnung, L., Kaasinen, E., Sahu, B., Yin, Y., Wei, B., Dodonova, S.O., Nitta, K.R., Morgunova, E., Taipale, M.*, et al.* (2018). The interaction landscape between transcription factors and the nucleosome. Nature *562*, 76-81.